Ecology, 99(11), 2018, pp. 2558–2574

Organic matter and nutrient inputs from large wildlife influence ecosystem function in the Mara River, Africa

Amanda L. Subalusky [1,2,4] Christopher L. Dutton [1] Laban Njoroge [3] Emma J. Rosi [2] and David M. Post [1]

[1]*Department of Ecology and Evolutionary Biology, Yale University, New Haven, Connecticut 06511 USA*
[2]*Cary Institute of Ecosystem Studies, Millbrook, New York 12545 USA*
[3]*Invertebrate Zoology Section, National Museums of Kenya, Nairobi, Kenya*

Abstract. Animals can be important vectors for the movement of resources across ecosystem boundaries. Animals add resources to ecosystems primarily through egestion, excretion, and carcasses, and the stoichiometry and bioavailability of these inputs likely interact with characteristics of the recipient ecosystem to determine their effects on ecosystem function. We studied the influence of hippopotamus excretion/egestion and wildebeest carcasses, and their interactions with discharge, in the Mara River, Kenya. We measured nutrient dissolution and decomposition rates of wildlife inputs, the influence of inputs on nutrient concentrations and nutrient limitation in the river and the influence of inputs on biofilm growth and function in both experimental streams and along a gradient of inputs in the river. We found that hippopotamus excretion/egestion increases ammonium and coarse particulate organic matter in the river, and wildebeest carcasses increase ammonium, soluble reactive phosphorus, and total phosphorus. Concentrations of dissolved carbon and nutrients in the water column increased along a gradient of wildlife inputs and during low discharge, although concentrations of particulate carbon decreased during low discharge due to deposition on the river bottom. Autotrophs were nitrogen limited and heterotrophs were carbon limited and nitrogen and phosphorus colimited upstream of animal inputs but there was no nutrient limitation downstream of inputs. In experimental streams, hippo and wildebeest inputs together increased biofilm gross primary production (GPP) and respiration (R). These results differed in the river, where low concentrations of hippo inputs increased gross primary production (GPP) and respiration (R) of biofilms, but high concentrations of hippo inputs in conjunction with wildebeest inputs decreased GPP. Our research shows that inputs from large wildlife alleviate nutrient limitation and stimulate ecosystem metabolism in the Mara River and that the extent to which these inputs subsidize the ecosystem is mediated by the quantity and quality of inputs and discharge of the river ecosystem. Thus, animal inputs provide an important ecological subsidy to this river, and animal inputs were likely important in many other rivers prior to the widespread extirpation of large wildlife.

Key words: carcass; discharge; ecosystem function; egestion; excretion; hippopotamus; productivity; river; Serengeti-Mara Ecosystem; stoichiometry; subsidy; wildebeest.

Introduction

Animals are important vectors for the movement of carbon and nutrients among ecosystems (Kitchell et al. 1979, Vanni 2002, Atkinson et al. 2016), and these animal inputs can act as subsidies that influence the dynamics of the recipient ecosystem (Polis et al. 1997, Anderson et al. 2008; Subalusky and Post 2018). Resource subsidies can strongly affect nutrient cycling (Kitchell et al. 1999, Atkinson et al. 2016), ecosystem productivity (Marcarelli et al. 2011, Samways and Cunjak 2015), and food web structure and stability (Huxel and McCann 1998, Leroux and Loreau 2008). Animals are particularly important subsidy vectors because they can create hotspots and hot moments of carbon and nutrient cycling when animals aggregate in time and space (McClain et al. 2003, McIntyre et al. 2008), transport carbon and nutrients against naturally established gradients (e.g., upstream or upslope; Naiman et al. 2009), or supply limiting carbon and nutrients (Vanni 2002).

There are two primary forms in which animals input organic matter and nutrients into recipient ecosystems: carcasses and waste excretion/egestion (Kitchell et al. 1979, Vanni 2002; Subalusky and Post 2018). When animals die in a recipient ecosystem, the carcass decomposes, providing a complex source of carbon and nutrients (Polis and Hurd 1996, Wipfli et al. 1998, Smith and Baco 2003, Menninger et al. 2008, Walters et al. 2009). When animals spend time in a recipient ecosystem after feeding elsewhere, they contribute carbon and nutrients to that ecosystem through excretion of soluble organic and inorganic nutrients from assimilated resources and egestion of particulate carbon and nutrients from consumed but not assimilated resources (Meyer and Schultz 1985, Post et al. 1998, Vanni 2002, Janetski et al. 2009, Post and Walters 2009, Roman and McCarthy 2010). Differences in stoichiometry and bioavailability between these different forms of input can influence their effects on aspects of ecosystem function, such as decomposition, nutrient cycling, and the balance between primary production of autochthonous carbon and microbial respiration of allochthonous carbon (Marcarelli et al. 2011, Tiegs et al. 2011, Sitters et al. 2015; Subalusky and Post 2018).

Manuscript received 6 March 2018; revised 19 July 2018; accepted 27 July 2018. Corresponding Editor: Christopher C. Wilmers.
[4] E-mail: asubalusky@gmail.com

The effects of inputs on ecosystem function are also mediated by characteristics of the recipient ecosystem (Polis et al. 1997, Marczak et al. 2007, Richardson et al. 2010, Atkinson et al. 2016). In rivers, discharge is a master variable that influences ecosystem size, retention rate, nutrient uptake, organic matter flux, and light availability (Power et al. 1995, Gibson and Meyer 2007, Tank et al. 2008). Thus, discharge likely interacts strongly with the form of animal input to influence the extent to which these inputs affect river ecosystem dynamics (Janetski et al. 2009, Tiegs et al. 2011, Dutton et al. 2018*b*, Stears et al. 2018). Productivity and resource availability within the recipient ecosystem also may influence the way animal inputs are processed and utilized (Witman et al. 2004, Marczak et al. 2007, Paetzold et al. 2008; Subalusky and Post 2018).

We tested the interacting effects of animal input form and discharge in the Mara River of East Africa. The Mara River ecosystem contains a population of over 4,000 hippos (*Hippopotamus amphibius*) (Kanga et al. 2011) and is on the route of the largest remaining overland migration in the world of 1.3 million wildebeest (*Connochaetes taurinus*; Hopcraft et al. 2013). Hippos consume grass from the surrounding savanna during nighttime feeding migrations and spend their day basking in the river, transporting terrestrial carbon and nutrients through excretion and egestion (Eltringham 1999, Subalusky et al. 2015). Modeling estimates suggest hippos in the Mara basin contribute 3,125 Mg dry mass (DM) to the river every year, and excretion accounts for 70% of the nitrogen (N) and 33% of the phosphorus (P) in these inputs (Subalusky et al. 2015). In other systems where animal excretion inputs have been studied, excretion increases the concentration of inorganic nutrients (Meyer and Schultz 1985, Post et al. 1998, Janetski et al. 2009), the rate of nutrient cycling (Kitchell et al. 1979, Vanni 2002, McIntyre et al. 2008), and primary production (Childress et al. 2014). Hippo egestion accounts for 88% of total carbon (C) inputs from hippos, and these carbon inputs may play a similar role as leaf litter in headwater streams in stimulating microbial processes (Webster and Benfield 1986, Webster et al. 1999), especially since hippo feces contain large particulates that settle on the river bottom. Hippo inputs also have finer particulates that increase turbidity in the river (Dutton et al. 2013, 2018*a*), which may reduce light penetration and limit primary production, thus influencing the physical characteristics of the recipient ecosystem. Hippo inputs occur in the river throughout the year, although their magnitude can vary seasonally as a function of resource quality and time spent grazing outside the river (Eltringham 1999, Kanga et al. 2013, Subalusky et al. 2015). The relative magnitude and ecological effects of hippo inputs are also largely influenced by fluctuations in river discharge that concentrate inputs during low discharge and dilute them during high discharge (Masese et al. 2015, 2018, McCauley et al. 2015, Dutton et al. 2018*b*, Stears et al. 2018)

Wildebeest migrate seasonally across the greater Serengeti-Mara Ecosystem, and they cross the Mara River at several regular crossing sites primarily in Kenya. At these crossings, periodic drownings of wildebeest can lead to the input of large numbers of carcasses (Dechant-Boaz 1982, Subalusky et al. 2017). We estimate an average of 6,250 carcasses enter the river each year, contributing 301 tons DM annually (Subalusky et al. 2017). Ninety-five percent of the P is in the skeleton, which decomposes over 7.4 yr, while 75% of the N is in soft tissue, which decomposes over 0.5–2.5 months (Subalusky et al. 2017). Wildebeest carcasses are a high-quality resource, with a low C to nutrient ratio, and likely play a similar role in the Mara River as fish carcasses do in other rivers where fish life cycles lead to large seasonal inputs of carcasses. Carcass inputs are typically associated with increased primary production (Wipfli et al. 1998, Naiman et al. 2009, Samways and Cunjak 2015); however, they have also been shown to stimulate increases in heterotrophic activity (Menninger et al. 2008), particularly in combination with scouring of biofilms from increased animal activity associated with spawning (Holtgrieve and Schindler 2011). Wildebeest carcasses enter the Mara during a season of relatively high discharge. River crossings and drownings occur from July to November, and the latter part of that time frame overlaps with the "short rain" season. Although our research has not shown a strong relationship between carcass inputs and discharge (Subalusky et al. 2017), higher average discharge during this season may mitigate carcass effects on ecosystem function. Wildebeest carcasses also enter the river in a region already influenced by large numbers of hippos and their associated inputs, which may further influence carcass effects on the river ecosystem.

The Mara River provides a unique opportunity to investigate the distinct effects of the two primary forms of animal input because of the occurrence of two animal vectors that vary in the timing and form of their inputs (Fig. 1). The different timing and composition of these inputs likely leads to different effects on ecosystem processes. Large inputs of allochthonous organic material, such as that provided by hippo feces and wildebeest carcasses, often drive aquatic ecosystems to become net heterotrophic through high rates of microbial respiration and promote production through the detrital food chain (Tank et al. 2010, Marcarelli et al. 2011). However, mineralization of that material may increase inorganic nutrient concentrations in the river and increase primary production (Naiman et al. 2009). Nutrient-rich inputs, such as hippo urine, also may increase autotrophic production, particularly when they occur during low discharge when light limitation associated with turbidity and depth is reduced (Young and Huryn 1996, Roberts and Howarth 2006). Thus, depending on input form and environmental context, allochthonous inputs may increase rates of nutrient cycling, alleviate nutrient limitation, stimulate primary production, and/or promote microbial processing of particulate organic matter (Roberts and Howarth 2006, Levi et al. 2013, Kominoski et al. 2015, Rosemond et al. 2015).

In this study, we used multiple approaches at different scales to explore how hippo and wildebeest inputs, alone and with one another, interact with river ecosystem characteristics to influence ecosystem function. We used small-scale chamber experiments and in situ decomposition experiments to quantify mineralization rates for different forms of animal input. We used field measurements to quantify the influence of hippo and wildebeest inputs on carbon and nutrient concentrations in the river across variable discharge levels, and we conducted *in situ* nutrient limitation assays to examine whether nutrient inputs altered nutrient limitation of auto- and/or heterotrophs. Finally, we measured biofilm growth,

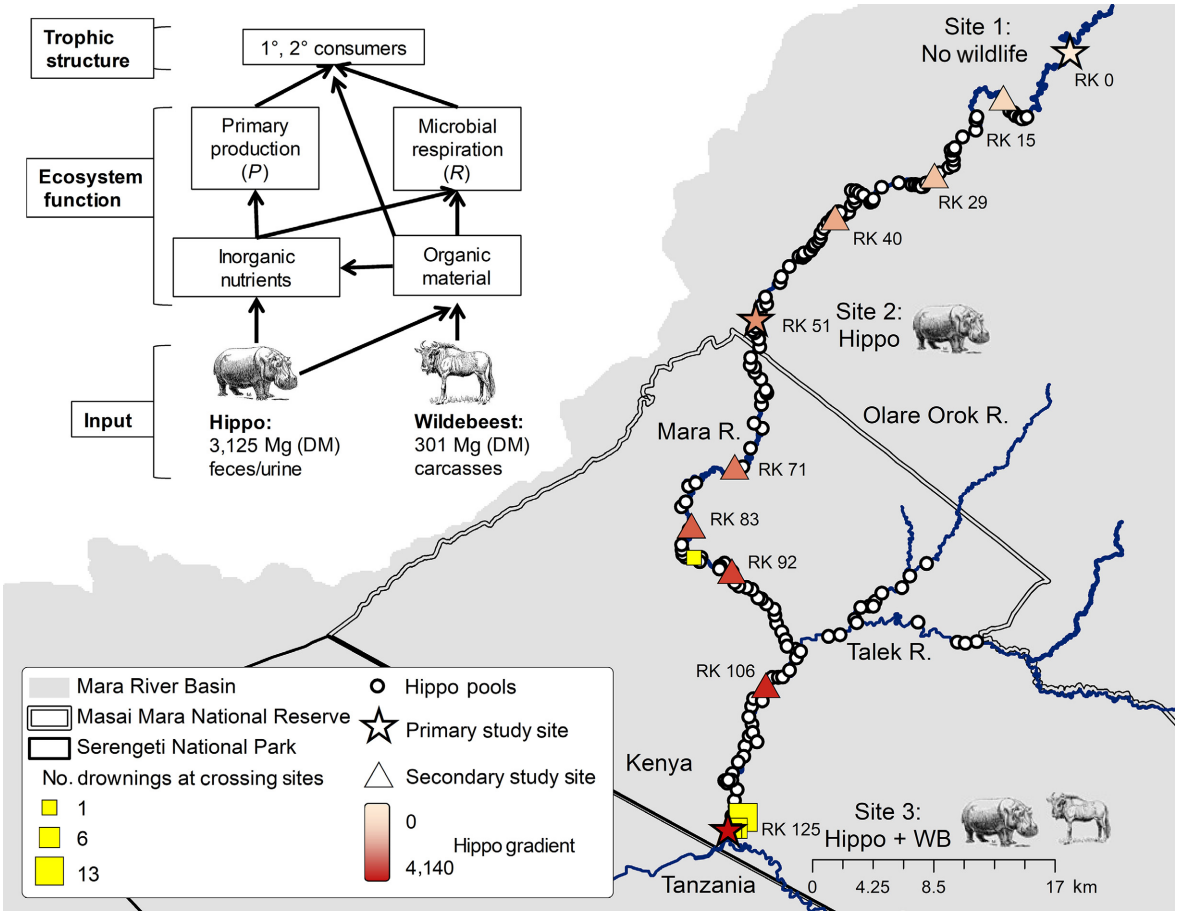

FIG. 1. Study region on the Mara River, which flows through the Maasai Mara National Reserve (MMNR) in Kenya and Serengeti National Park (SNP) in Tanzania. Primary study sites are labeled according to wildlife input; primary and secondary study sites are labeled according to distance from Site 1 in river km. Hippo pools are mapped according to Kanga et al. (2011), and wildebeest (WB) drownings are mapped following Subalusky et al. (2017). Site 1: No Wildlife is downstream of most human settlement in the basin and upstream of all large wildlife populations. Site 2: Hippo is downstream of ~1,590 hippos and upstream of wildebeest crossing sites. Site 3: Hippo + WB is downstream of a total of ~4,140 hippos and all wildebeest crossing and drowning locations. The inset conceptual figure, from Subalusky and Post (2018), illustrates the two forms of wildlife input and predicted pathways through which they influence ecosystem function and trophic structure.

GPP, and *R* in experimental streams and in situ to examine how different forms of input influence autotrophic and heterotrophic production. We hypothesized that hippo inputs would increase carbon and nitrogen concentrations in the river and primarily drive the river towards increasing heterotrophy and that wildebeest inputs would increase nitrogen and phosphorus concentrations in the river and increase autotrophy. However, because carcasses enter the river during relatively high discharge, and at a location where the river has high particulate carbon concentrations due to hippo inputs, we also posed the alternative hypothesis that carcasses may stimulate heterotrophic rather than autotrophic activity.

METHODS

Study sites

The Mara River is a trans-boundary river that flows from forested headwaters in Kenya through the Masai Mara National Reserve (MMNR) and Serengeti National Park (SNP) before entering Lake Victoria in Tanzania (Fig. 1). Our uppermost study site, Site 1, is at Emarti Bridge, just downstream of the confluence of the upper two tributaries that form the Mara River, and land use upstream is predominantly small-scale subsistence agriculture with some large-scale farming (Hoffman 2007, Mati et al. 2008). Site 2 is located at the Narok-Lolgorien Bridge (Old Mara Bridge) just upstream of the MMNR, and land use between Sites 1 and 2 is predominantly open rangelands used by Maasai pastoralists with some tourism development. Site 3 is located at the Purungat Bridge (New Mara Bridge) just upstream of the Kenya-Tanzania border, and land use between Sites 2 and 3 is largely within the MMNR with abundant large wildlife and a number of tourist lodges.

There are essentially no large wildlife populations upstream of Site 1. The hippo population begins just downstream of Site 1, and there are ~170 hippo pools relatively evenly distributed throughout the remaining study sites. There are approximately 1,590 hippos upstream of Site 2, and 4,140 hippos upstream of Site 3 (inclusive of those upstream of Site 2 and in the Talek River sub-catchment;

Kanga et al. 2011). Due to migratory pathways, all wildebeest river crossings and related drownings occur between Sites 2 and 3 from July to November (Subalusky et al. 2017). These spatial and temporal patterns in animal inputs allowed us to measure the Mara with no wildlife inputs at Site 1 (hereafter No Wildlife); with low concentrations of hippo inputs at Site 2 (Hippo); and with high concentrations of hippo inputs and wildebeest inputs at Site 3 (Hippo + WB), which we can measure with fresh carcasses from July to November and without fresh carcasses from December to June (Fig. 1).

Our earlier research estimated the magnitude and stoichiometry of hippo and wildebeest inputs into the Mara River (Subalusky et al. 2015, 2017) (Table 1). For these measurements, and for all the experiments detailed herein, we collected fresh hippo feces in the morning within a day of use for each experiment and stored it until use in a covered plastic bin to maintain moisture content. We collected wildebeest tissue from freshly drowned wildebeest carcasses that we pulled from the river (1 adult male and 1 sub-adult male in 2012, and 1 adult female in 2013). Wildebeest tissue from these carcasses was stored in a freezer until needed for experiments.

We measured discharge for the Mara River over the course of our study (2011–2014) at the No Wildlife site and the Hippo + WB site using depth transducers corrected with barometric pressure loggers (In-Situ, Fort Collins, Colorado, USA; Eureka Water Probes, Austin, Texas, USA). Stage heights were converted to discharge using rating curves that we developed for each site using the velocity–area method (Herschy 1998). Outliers were removed from the rating curves if they both fell outside the 95% confidence intervals and were collected during the rising or falling limb of floods. A more detailed description of our discharge measurements and rating curves is in Dutton et al. (2018*a*). The Mara River is characterized by a bimodal hydrological cycle, with long rains from March to June and short rains from October to December. Base flow discharge at the Hippo + WB site was lower on average than at the No Wildlife site, although the Hippo + WB site had larger and more frequent high discharge events associated with rain, likely due to large rain events in the Talek River sub-catchment (Dutton et al. 2018*a*). Mean discharge at the No Wildlife site over the course of our study was 15.6 m^3/s, and it ranged from 0.8 to 116.3 m^3/s. Mean discharge at the Hippo + WB site over the period of measurement was 11.8 m^3/s, and it ranged from 0.8 to 196.6 m^3/s.

Nutrient dissolution rates

We used chamber experiments to measure net carbon and nutrient dissolution rates of hippo feces and wildebeest muscle tissue and their influence on community respiration. We used 5-L chambers filled with river water, and we created three replicates of each of six treatments: control, low (1 g), medium (5 g), and high (20 g) concentrations of hippo feces, wildebeest muscle (26 g), and hippo feces (5 g) + wildebeest muscle (26 g). We collected subsamples of water for nutrient analysis at 24, 71, and 133 h. Samples were analyzed in the field for ammonium (NH_4^+-N) using fluorometric methods (Holmes et al. 1999, Taylor et al. 2007), and then acidified and transported to the lab for analysis of soluble reactive phosphorus (SRP) using the molybdate blue method (APHA 2006). We measured dissolved organic carbon (DOC) in samples that we filtered through Whatman GF/F filters, acidified to pH < 2 and analyzed on a Shimadzu total organic carbon analyzer (Shimadzu, Kyoto, Japan). Sample values from the controls (i.e., replicates with nothing added) were subtracted from treatment sample values to correct for background concentration, and corrected concentrations were multiplied by the volume of water in the chamber to yield total amount. We estimated community respiration by measuring dissolved oxygen (DO) using an optical probe (ProODO; YSI, Yellow Springs, Ohio, USA) in each of the chambers at each sampling point and correcting for DO concentrations in the control samples.

Some values were negative after being corrected for control concentrations, so we standardized all values to make the lowest value positive, and we transformed the data using log-transformations. We analyzed each of the four response variables (NH_4, SRP, DOC, and DO) in response to treatment and time using repeated-measures (rm) ANOVA with the aov

Table 1. Estimated magnitude, stoichiometry, and decomposition rate of different components of inputs from hippos (urine and feces) and wildebeest (soft tissue and bone) into the Mara River, Kenya.

Input	Mass (mean ± SD Mg dry mass/yr)	Stoichiometry (C:N:P by mass)	Decay rate (mean ± SE)	Days to 95% loss	Input at Site 2:Hippo (daily input of C:N:P in kg)	Input at Site 3:Hippo + WB (daily input of C:N:P in kg)
Hippo urine (zoo)†	–	25.8:15.8:1.0				
Hippo feces (zoo)†	–	96.5:3.4:1.0				
Hippo feces (field)†,‡	3,125	222.8:6.3:1.0	–0.038 ± 0.002	80	1327:187:18	3499:492:48
Wildebeest soft tissue§	169 ± 81	127.0:31.0:1.0	–0.043 ± 0.002 –0.188 ± 0.009	16–70		2288:558:18¶
Wildebeest bone§	132 ± 63	2.6:0.5:1.0	–0.001 ± 0.000	2723		12:2:4¶

†Hippo input mass and stoichiometry data from Subalusky et al. (2015).
‡Decomposition rate data based on fresh feces measured in this study.
§Wildebeest data from Subalusky et al. (2017); decay rate reflects range from skin to meat.
¶Daily rates for wildebeest inputs are estimated based on the total annual inputs divided by the average days to decay.

function in R (R Core Team 2018). If there was a significant treatment effect at $\alpha = 0.05$, we then performed a Tukey pairwise comparison test between treatments using the Holm method to adjust *P* values for multiple comparisons (Holm 1979, R Core Team 2018). All statistical analyses in this paper were done in R version 3.3.2 (R Core Team 2018).

Decomposition rates

We used fine mesh litterbags (mesh size <500 μm) to measure the decomposition rate of hippo feces in the river under three different conditions: fresh hippo feces (simulating hippo feces input directly to the river), aged hippo feces (fresh feces that were washed and dried to simulate the effects of rain and sun on hippo feces first deposited on land and then washed into the river), and aged hippo feces + wildebeest muscle tissue (simulating hippo feces in the river with fresh wildebeest carcasses present). We used 40 g (wet mass) of fresh hippo feces, 10 g (dry mass) of aged hippo feces to approximate a similar quantity as fresh hippo feces, since previous research has shown the percent dry mass is typically ~25%, and 20 g of wildebeest muscle tissue. We prepared 36 replicates of each treatment.

We attached the litterbags to a heavy chain that we secured to the bottom of the river at the Hippo + WB site. We collected three replicates immediately after deploying the litterbags to estimate the mass loss during deployment, and we collected three replicates every 2–14 d over 63 d. Upon retrieving a litterbag, we removed the hippo feces, washed it in a 1 mm sieve to remove dirt and sand that had accumulated in the bag, dried it to constant mass and determined its dry mass.

For each time period, we calculated percentage of mass remaining and we used a single-slope exponential decay function to calculate mass loss over time (Wider and Lang 1982, Regester and Whiles 2006): $\ln(x_t) = \ln(x_0) - kt$, where x_t is the mass remaining at time t, x_0 is the initial mass, and $-k$ is the slope of the ln-transformed decay equation and the decay constant. We adjusted all models so that x_t/x_0 equals 100% at time 0. We calculated days to 95% mass loss by dividing ln 0.05 by $-k$. We used a two-way ANOVA to analyze the influence of treatment (fresh, aged, with wildebeest) on decay rate (R Core Team 2018). Presence of an interaction effect between treatment and time at $\alpha = 0.05$ indicated a significant effect of treatment on decay rate. We then conducted pairwise analyses of each treatment combination using one-way ANOVAs to determine how they differed from one another. We accounted for the number of pairwise comparison tests by using a Bonferroni adjusted α value of 0.0167 to indicate statistical significance.

River physicochemical parameters

We measured temperature, turbidity, dissolved oxygen, specific conductivity, salinity, total dissolved solids, and pH every 15 min at the No Wildlife site and the Hippo + WB site throughout the period of study with Eureka Manta2 sondes (Eureka Water Probes). We collected water samples for nutrient analysis twice monthly at each of the three primary study sites from June to August 2011, and monthly from July to December 2012 and August 2013–April 2014. To confirm that our primary study sites were reflective of the overall trend from up- to downstream, we also collected water samples along a 10-point transect of secondary study sites distributed from the No Wildlife site to the Hippo + WB site once during high flows (November 2013) and once during low flows (February 2014). Water samples were kept cold (<4°C) after collection, filtered within 12 h, and acidified or frozen within 24 h.

We measured total nitrogen (TN) and total phosphorus (TP) concentrations in unfiltered samples using an alkaline potassium persulfate digestion reagent. We measured NH_4^+-N concentrations in the field using fluorometric methods in 2011–2012 (Holmes et al. 1999, Taylor et al. 2007) and using the gas exchange method in 2013–2014 (APHA 2006). We measured nitrate + nitrite (NO_3^--N+NO_2^--N) concentrations using cadmium reduction in 2011 and using zinc reduction in 2012–2014 (APHA 2006, Ellis et al. 2011). We measured SRP and DOC as described in *Nutrient dissolution rates*.

We measured total suspended solids (TSS) by filtering a known volume of sample through a pre-weighed Whatman GF/F filter, drying the filter at 60°C and re-weighing it. We measured ash-free dry mass (AFDM) by combusting the GF/F filter at 450°C and then re-weighing it to determine mass loss upon combustion. We collected coarse particulate organic matter (CPOM) with a 1-mm mesh net, and we calculated concentrations based on the volume of water that passed through the net. CPOM samples were air-dried in the field until completely dry and weighed on a balance (Scout Pro 600 g; Ohaus, Parsippany New Jersey, USA).

We used non-parametric statistics due to the non-normal distribution of several parameters that could not be addressed through transformation and the presence of outliers in the data. We used a Kruskal-Wallis test to examine differences in nutrient and carbon concentrations between sites (R Core Team 2018). We then used a Dunn's test for post hoc pairwise comparisons with unequal sample sizes, and we used a Holm adjusted *P* value to account for multiple comparisons (Holm 1979, Dinno 2016). We multiplied concentration by discharge to obtain flux estimates (kg/d), and we analyzed differences in nutrient flux by site with and without the presence of wildebeest carcasses. We classified sample dates as being in the wildebeest season if carcasses had been detected upstream of the Hippo + WB site within one month prior to the sampling date. We used a Mann-Whitney *U* test to test for differences in flux by season at the three sites (R Core Team 2018). The only significant difference by season was for TN at the No Wildlife site ($P = 0.04$), so we combined data from all sampling dates for the No Wildlife site and for the Hippo site. We then used a Kruskal-Wallis test followed by Dunn's test for pairwise comparisons with a Holm adjusted *P* value to test for flux differences between the No Wildlife site, the Hippo site, the Hippo + WB site with carcasses, and the Hippo + WB site without carcasses (Holm 1979, Dinno 2016, R Core Team 2018). We then compared C, N, and P flux estimates at these sites to our estimates of wildlife inputs from prior research (Table 1, Appendix S1; Subalusky et al. 2015, 2017).

Nutrient limitation

We used nutrient diffusing substrates (NDSs) to measure benthic nutrient limitation at our three primary study sites

in 2011 and 2013 (Tank et al. 2007, 2017). We used inorganic (fritted glass) substrates to measure autotrophic community response and organic (cellulose sponge) substrates to measure heterotrophic community response. Substrates were placed on agar amended with nutrients and placed in a flowing section of river for several weeks. In 2011, we analyzed six treatments on each substrate with five replicates each: ammonium chloride (NH_4Cl), potassium phosphate (KH_2PO_4), sodium nitrate ($NaNO_3$), NH_4Cl + KH_2PO_4, $NaNO_3$ + KH_2PO_4, and a control. All nutrients were added to the agar at 0.5 mol/L. The NDSs were deployed from 5 to 29 July 2011, for 21 d each. On 14 July, a large wildebeest drowning of 5,000 individuals occurred 38 km upstream of the Hippo + WB site, and elevated nutrient levels were detected at the site from this event. In 2013, we analyzed the same six treatments, as well as sodium acetate ($C_2H_3NaO_2$) as a complex source of carbon, on each substrate with five replicates each. The NDSs were deployed from 27 August to 13 September 2013, for 15 d at each site. There were wildebeest drownings on 20 August 2013, and there were approximately 1,000 carcasses in the river within 3.6 km upstream of the Hippo + WB site during the deployment.

In both years, we measured chlorophyll *a* (chl *a*) of biofilms on inorganic substrates and respiration (*R*) of biofilms on organic substrates after NDSs were collected in the field. The inorganic substrates were frozen for >24 h; chl *a* was extracted using methanol with a basic pH (Holm-Hansen 1978), and samples were analyzed on a Turner Aquafluor handheld fluorometer (Turner Designs, Sunnyvale, California, USA). We measured *R* by placing the organic substrates into 50-mL Falcon tubes filled with stream water and no air bubbles and measuring oxygen consumption during dark treatments using an optical dissolved oxygen probe (ProODO; YSI). We used stream water controls to correct for changes in background DO levels (Hoellein et al. 2010). Data were square-root-transformed to meet assumptions of normality. We used a two-way ANOVA to analyze the response of biofilms to different nutrient treatments at different sites in both 2011 and 2013. If there were significant interactions at $\alpha = 0.05$, we used one-way ANOVAs to analyze treatment responses separately for each site, followed by Tukey's HSD post hoc test for multiple comparisons (R Core Team 2018).

Ecosystem function

Experimental streams.—We used recirculating experimental stream channels to test the influence of both hippo and wildebeest inputs on biofilm growth, primary production, and respiration (Appendix S2: Fig. S1). Stream channels were constructed out of PVC canvas. The channel length was 4.2 m long and 19 cm wide. Streams were filled with 60 L water from the Amala River, which is a tributary of the Mara upstream of wildlife influence. Water was recirculated by a paddle wheel affixed to a shaft, which was turned by a motor, with each of two shafts recirculating the water for a block of six streams. We replaced 50% of the volume of water in the streams each day. The streams were located outside under the shade of a large tree, and the entire array was covered with a shade cloth to minimize spatial variability in incident light among streams.

We used three replicates each of four treatments: control, hippo, wildebeest (WB), and hippo + wildebeest (Hippo + WB). Treatments were randomly assigned among each block of experimental streams. Each week, we added 10 g (wet mass) of fresh hippo feces to the Hippo and Hippo + WB treatments and we added 10 g muscle tissue to the WB and Hippo + WB treatments. The inputs were placed in fine mesh bags (mesh size < 500 μm) and suspended in the flowing water so that they could be removed and replaced with fresh material each week.

Streams were lined with washed gravel rock, and five unglazed ceramic tiles were placed in each channel for sampling biofilms. Each week, we removed one tile from each stream and measured biofilm GPP, *R*, and biomass. We measured GPP and *R* using watertight clear plastic boxes as incubation chambers. We measured net ecosystem production (NEP) as oxygen production during light treatments and respiration (*R*) as oxygen consumption during dark treatments using an optical dissolved oxygen probe (ProODO meter; YSI). We used stream water controls to correct for changes in background dissolved oxygen levels (DO). We calculated gross primary production (GPP) as the sum of NEP and *R* (Hoellein et al. 2010). Biofilm quantity was measured by scrubbing the biofilm off each tile into a small volume of water and filtering known volumes of the water through two replicate Whatman GF/F filters. One filter was dried, weighed, combusted at 450°C for 2 h and re-weighed to measured organic matter as ash-free dry mass (AFDM). The other filter was analyzed for chl *a* as described in *Nutrient limitation* (Holm-Hansen 1978). We measured biofilm growth weekly over four weeks.

We transformed the data to meet the assumptions of normality using log-transformations for GPP and *R* and square-root transformations for AFDM and chl *a*. We analyzed each of the four response variables (GPP, *R*, AFDM, and chl *a*) throughout the duration of the experiment using a linear mixed-effect model run with the lme function in the nlme package in R (Pinheiro et al. 2016, R Core Team 2018). We fitted lme models with the restricted maximum likelihood method and a continuous autoregressive temporal correlation structure with day as the repeated factor. Treatment (Control, Hippo, WB, Hippo + WB) and time (each of 4 weeks of measurement) were treated as fixed effects, and individual streams were treated as random effects. A significant interaction between treatment and time indicated different rates of biofilm growth by treatment. We then used lstrends in the lsmeans package to perform a Tukey pairwise comparison test between treatments for biofilm parameters over the duration of the experiment (Lenth 2016, R Core Team 2018). We also used one-way ANOVAs to analyze differences in standing stock biofilm parameters by treatment in the final week of the experiment.

River biofilms.—From 2012 to 2014, we measured the accrual and activity of epilithic biofilms at our three primary study sites. To mimic rocks in the river, we placed five unglazed ceramic tiles at each site monthly and allowed epilithic communities to grow for at least three weeks prior to sampling. We scraped the top surface of the tiles and measured chl *a* and AFDM as previously described. In 2013–

2014, prior to scraping off the biofilm, we also measured GPP and *R* on each tile as previously described. Data were normally distributed with equal variance among sites, so we used a one-way ANOVA followed by Tukey's HSD test for pairwise comparisons to test for differences among sites (R Core Team 2018). We then used independent *t* tests to analyze differences in chl *a* and AFDM (for which we had sufficient data) by site with and without the presence of wildebeest carcasses at the Hippo + WB site. There were no significant differences between seasons for any of the three sites, so we then used a one-way ANOVA followed by Tukey's HSD test to test for differences between the No Wildlife site, the Hippo site, the Hippo + WB site with carcasses, and the Hippo + WB site without carcasses.

Water column.—From 2012 to 2014, we measured biomass, GPP, and *R* in the water column at our three primary study sites. We incubated five replicate water column samples in 300-mL glass bottles for 2–4 h in both light and dark conditions, and we measured NEP and *R* and calculated GPP as previously described. We estimated biochemical oxygen demand (BOD-5) in one additional bottle of river water, which was stored in water in the shade to maintain a relatively constant temperature around 20°C (lack of electricity precluded the use of an incubator), by subtracting initial DO from DO measured after 5 d (APHA 2006). We also measured nutrient concentrations, chl *a*, and AFDM. For chl *a* samples, water was pre-filtered using 500-μm mesh to remove large particulates. We analyzed the water column data using a Kruskal-Wallis ANOVA followed by Dunn's test for pairwise comparisons with a Holm adjusted *P* value to test for differences between sites (Holm 1979, Dinno 2016, R Core Team 2018).

Results

Nutrient dissolution rates

There were significant treatment effects of input type and concentration on NH_4 (rm ANOVA, $F_{4,35} = 23.53$, $P < 0.001$), SRP ($F_{4,35} = 123.61$, $P < 0.001$), and DOC ($F_{4,35} = 27.96$, $P < 0.001$), and significant treatment by time interaction effects on NH_4 (rm ANOVA, interaction, $F_{4,35} = 9.30$, $P < 0.001$) and SRP ($F_{4,35} = 7.59$, $P < 0.001$). Hippo feces rapidly leached SRP, DOC, and NH_4, which reached maximum concentrations within 24 h (Fig. 2). SRP and DOC stayed elevated throughout the experiment, while NH_4 declined below control concentrations by the fifth day, likely due to biogeochemical transformations and loss through nitrification and denitrification. Concentrations of NH_4, SRP, and DOC increased with increasing hippo feces concentration, although treatment differences were only significant for SRP and DOC (except for low and medium concentrations for DOC; pairwise *t* test, $P < 0.05$ for all comparisons). Wildebeest tissue continued to leach SRP and DOC throughout the course of the experiment, although NH_4 followed a similar pattern as for hippo feces. The wildebeest treatment was significantly higher in NH_4 than the lowest concentration of hippo feces ($P = 0.017$), and it was significantly higher in SRP and DOC than all

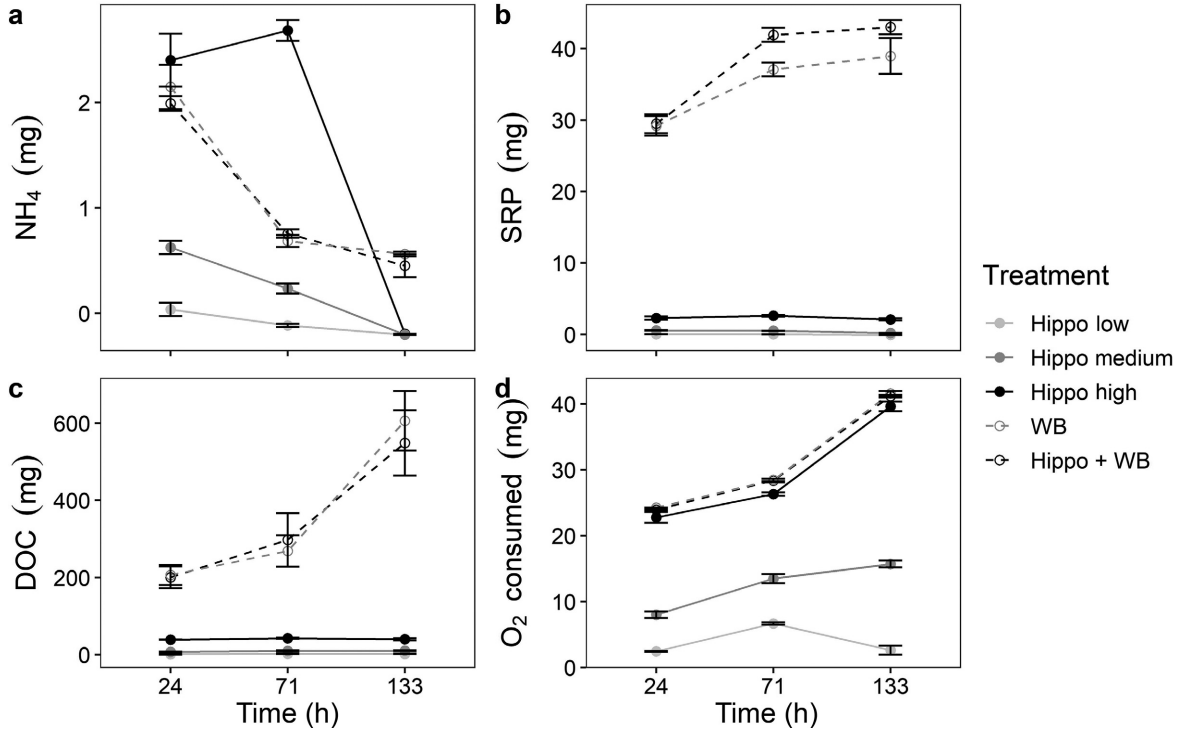

Fig. 2. Chamber experiments measuring the effect of different concentrations of hippo feces (Hippo low, 1 g; Hippo medium, 5 g; Hippo high, 20 g), wildebeest tissue (WB, 26 g) and both (Hippo + WB, 5 g hippo feces and 26 g wildebeest tissue) on mean (± SE) dissolution rates of (a) ammonium, (b) soluble reactive phosphorus, and (c) dissolved organic carbon, and (d) community respiration as indicated by oxygen consumption, in 5-L chambers over 5 d.

concentrations of hippo feces ($P < 0.05$ for all comparisons). Treatments with wildebeest tissue had around 20 times higher SRP concentrations and 15 times higher DOC concentrations than the highest hippo concentration by the end of the experiment, although NH_4 concentrations were lower until the end of the experiment. There were no significant differences between the WB and Hippo + WB treatments for NH_4 or DOC; however, SRP was higher in the Hippo + WB treatment as compared to the WB treatment ($P < 0.03$), and this difference was 10% greater than the summed SRP leached by Hippo and WB alone, suggesting a synergistic effect.

There were also significant treatment effects on DO (rm ANOVA, $F_{4,35} = 101.69$, $P < 0.001$). Both Hippo and WB treatments resulted in oxygen consumption throughout the course of the experiment. Oxygen consumption increased significantly with the concentration of hippo feces ($P < 0.05$ for all comparisons), and the slope of this relationship increased with concentration (although there was not a significant treatment by time interaction). There was no significant difference in oxygen consumption between the high concentration of hippo feces (Hippo), WB, and Hippo + WB treatments.

Decomposition rates

There was a significant interaction between the hippo feces treatment and time on the mass remaining (two-way ANOVA, interaction, $F_{2,75} = 3.19$, $P = 0.047$), indicating an effect of treatment on decay rate (Table 1, Appendix S2: Fig. S2). Fresh feces decayed faster than aged hippo feces (ANOVA, interaction, $F_{1,56} = 4.21$, $P = 0.045$), although this was not significant after accounting for multiple comparisons. There was no significant difference between decay rate of fresh feces and aged feces with carcass (ANOVA, interaction, $F_{1,49} = 0.18$, $P = 0.671$); however, aged feces with carcass decayed significantly faster than aged feces alone (ANOVA, interaction, $F_{1,45} = 8.20$, $P = 0.006$).

River physicochemical parameters

The Mara is a highly turbid river with high nutrient concentrations even above the influence of wildlife. Mean turbidity at our sites ranged from 266 to 440 NTU and mean NO_3 concentrations ranged from 877 to 958 μg/L (Appendix S2: Table S1). There was a general decline in water quality, as determined by physicochemical parameters, from upstream to downstream. Turbidity increased by 65%, conductivity increased by 24%, and DO decreased by 23% from the No Wildlife site to the Hippo + WB site (Appendix S2: Table S1).

Carbon and nutrient concentrations also increased from the No Wildlife site to the Hippo + WB site (Table 2). Concentrations of NH_4, SRP, TN, and DOC were significantly higher at the Hippo + WB site than at the No Wildlife and Hippo sites, but those two sites were not significantly different from one another (Table 3). Concentrations of TP and TSS increased significantly from the No Wildlife site to the Hippo site and from the Hippo site to the Hippo + WB site (Table 3). Concentrations of CPOM were higher at both the Hippo site and the Hippo + WB site than the No Wildlife site, although the Hippo and Hippo + WB sites were not significantly different from one another (Table 3). There were no significant differences in NO_3 by site (Table 3).

Flux of NH_4 at the Hippo + WB site was significantly higher than at the No Wildlife site both when wildebeest carcasses were present and when they were not, but they were only higher than at the Hippo site when carcasses were present (Fig. 3, Appendix S2: Table S2). Fluxes of SRP and TP were significantly higher at the Hippo + WB site than the No Wildlife site only with carcasses present (Fig. 3, Appendix S2: Table S2).

We found similar patterns in our higher spatial resolution sampling at secondary study sites (Fig. 4). Concentrations of NH_4, TN, DOC, and TP all increased from upstream (No Wildlife) to downstream (Hippo + WB), indicating that our three primary study sites are representative of a strong gradient of increasing wildlife inputs (Fig. 4). Concentrations of dissolved carbon and nutrients were consistently lower at all 10 sampling locations at high flow than low flow, suggesting dilution effects during high flows. In contrast, concentrations of CPOM were greatly elevated during high flows, suggesting increased mobilization of particulates during high flows.

River nutrient limitation

Respiration (R) by heterotrophic biofilms responded differently to nutrient treatments at sites with and without large

TABLE 2. Water column parameters measured from water samples collected monthly at the No Wildlife, Hippo, and Hippo + WB sites in the Mara River from June to August 2011, July to December 2012, and August 2013 to March 2014.

Site	Sample size (n)	NH_4 (μg/L)	NO_3 (μg/L)	TN (mg/L)	SRP (μg/L)	TP (μg/L)	DOC (mg/L)	TSS (mg/L)	CPOM (mg/L)	Chl *a* (μg/L)	AFDM (mg/L)	BOD5† (μg O_2/d)
No Wildlife	14–23	50.4 (86.3)	877.3 (121.8)	1.4 (0.8)	13.2 (12.4)	131.8 (132.6)	2.8 (1.0)	236.5 (364.6)	0.3 (0.5)	1.5 (2.0)	32.3 (44.6)	61.1 (32.5)
Hippo	13–23	62.6 (65.8)	907.6 (173.8)	1.8 (1.1)	15.9 (9.0)	190.8 (148.9)	3.3 (1.3)	276.1 (277.9)	1.4 (1.7)	3.7 (2.7)	39.1 (33.2)	118.0 (65.8)
Hippo+ WB	13–32	126.4 (107.8)	958.4 (179.8)	2.6 (1.4)	23.3 (11.0)	265.5 (191.3)	4.0 (1.3)	546.8 (619.3)	2.3 (3.6)	10.2 (17.1)	69.2 (71.0)	124.0 (27.5)

Notes: Mean values with standard deviation in parentheses are shown for ammonium (NH_4-N), nitrate (NO_3-N), total nitrogen (TN), soluble reactive phosphorus (SRP), total phosphorus (TP), dissolved organic carbon (DOC), total suspended solids (TSS), coarse particulate organic matter (CPOM), chlorophyll *a* (Chl *a*), ash-free dry mass (AFDM), and biochemical oxygen demand over 5 d (BOD5). Sample sizes varied for different parameters at each site.

†Sample size range for BOD5 was 5–8.

TABLE 3. Comparison of water column parameters at the No Wildlife, Hippo, and Hippo + WB sites in the Mara River from June to August 2011, July to December 2012, and August 2013 to March 2014 using a Kruskal-Wallis test followed by Dunn's test for pairwise comparisons with Holm adjustment when a significant site effect was present.

			P			
Nutrient concentration	Sample size (*n*)	χ^2	Site effect	No Wildlife : Hippo	Hippo : Hippo + WB	No Wildlife : Hippo + WB
NH_4 (μg/L)	18–25	16.40	**0.0003**	0.1148	**0.0079**	**0.0001**
NO_3 (μg/L)	23–32	3.15	0.2071			
SRP (μg/L)	22–32	14.56	**0.0007**	0.1012	**0.0214**	**0.0003**
TN (mg/L)	16–32	18.02	**0.0001**	0.0783	**0.0158**	**0.0001**
TP (μg/L)	16–32	19.07	**<0.0001**	**0.0379**	**0.0284**	**<0.0001**
DOC (mg/L)	23–32	16.67	**0.0002**	0.0694	**0.0162**	**0.0001**
TSS (mg/L)	21–28	15.36	**0.0005**	**0.0399**	**0.0453**	**0.0001**
CPOM (mg/L)	13–14	9.69	**0.0079**	**0.0134**	0.3560	**0.0066**
Chl *a* (μg/L)	21–29	33.05	**<0.0001**	**0.0005**	**0.0250**	**0.0000**
AFDM (mg/L)	21–28	14.99	**0.0006**	**0.0401**	0.0501	**0.0002**
BOD5 (μg O_2/d)	5–9	6.93	**0.0313**	0.0536	0.2520	**0.0221**

Notes: Significant *P* values are shown in boldface type. All χ^2 values have df = 2.

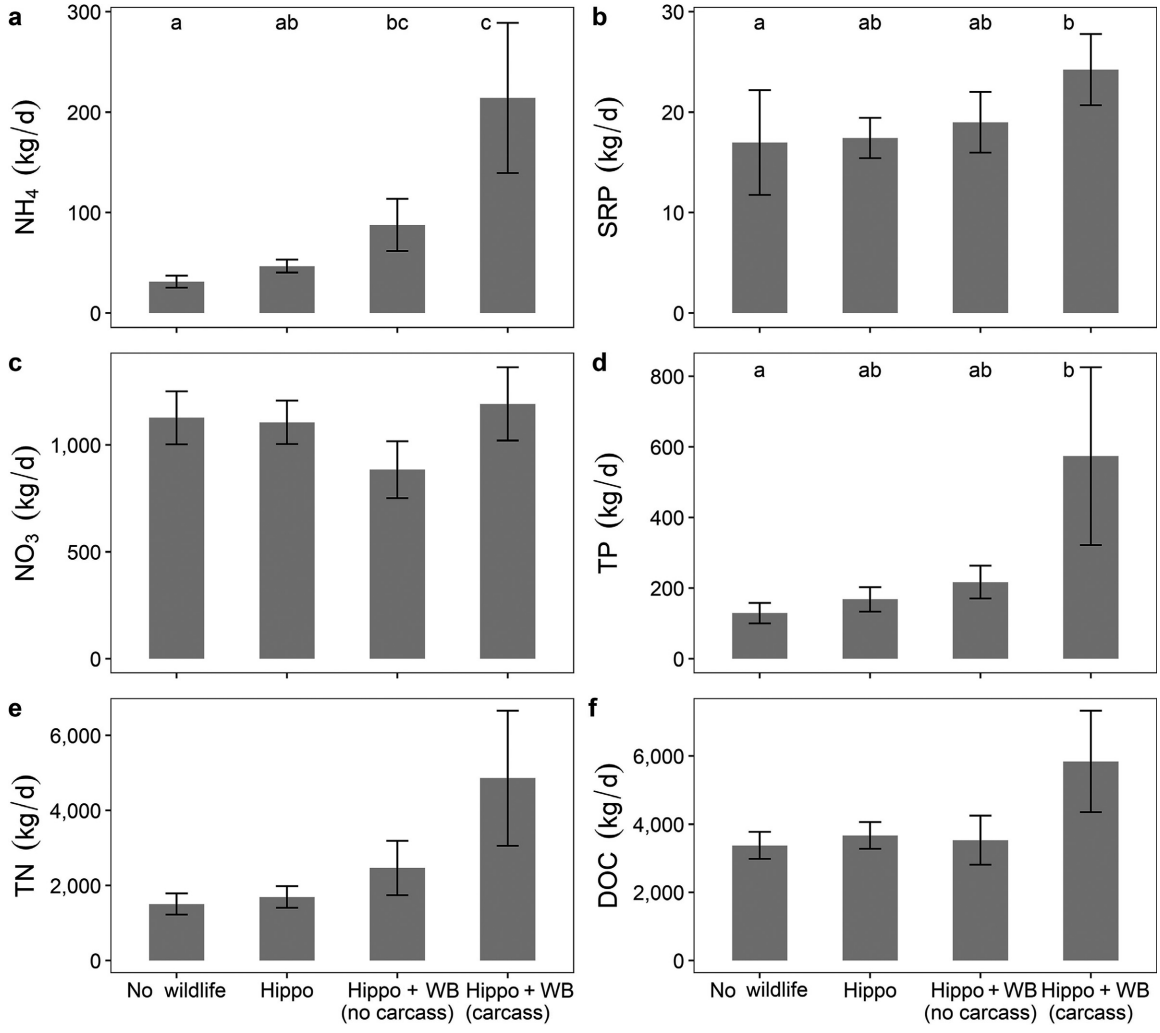

FIG. 3. Mean flux (± SE) of (a) ammonium, (b) soluble reactive phosphorus, (c) nitrate, (d) total phosphorus, (e) total nitrogen, and (f) dissolved organic carbon at the No Wildlife, Hippo, and Hippo + WB sites on the Mara River, Kenya, based on monthly or bimonthly sampling over the duration of the study from 2011 to 2014. Data for the Hippo + WB site is shown with and without the presence of fresh wildebeest carcasses. Lowercase letters above bars indicate significant differences among group means ($\alpha = 0.05$).

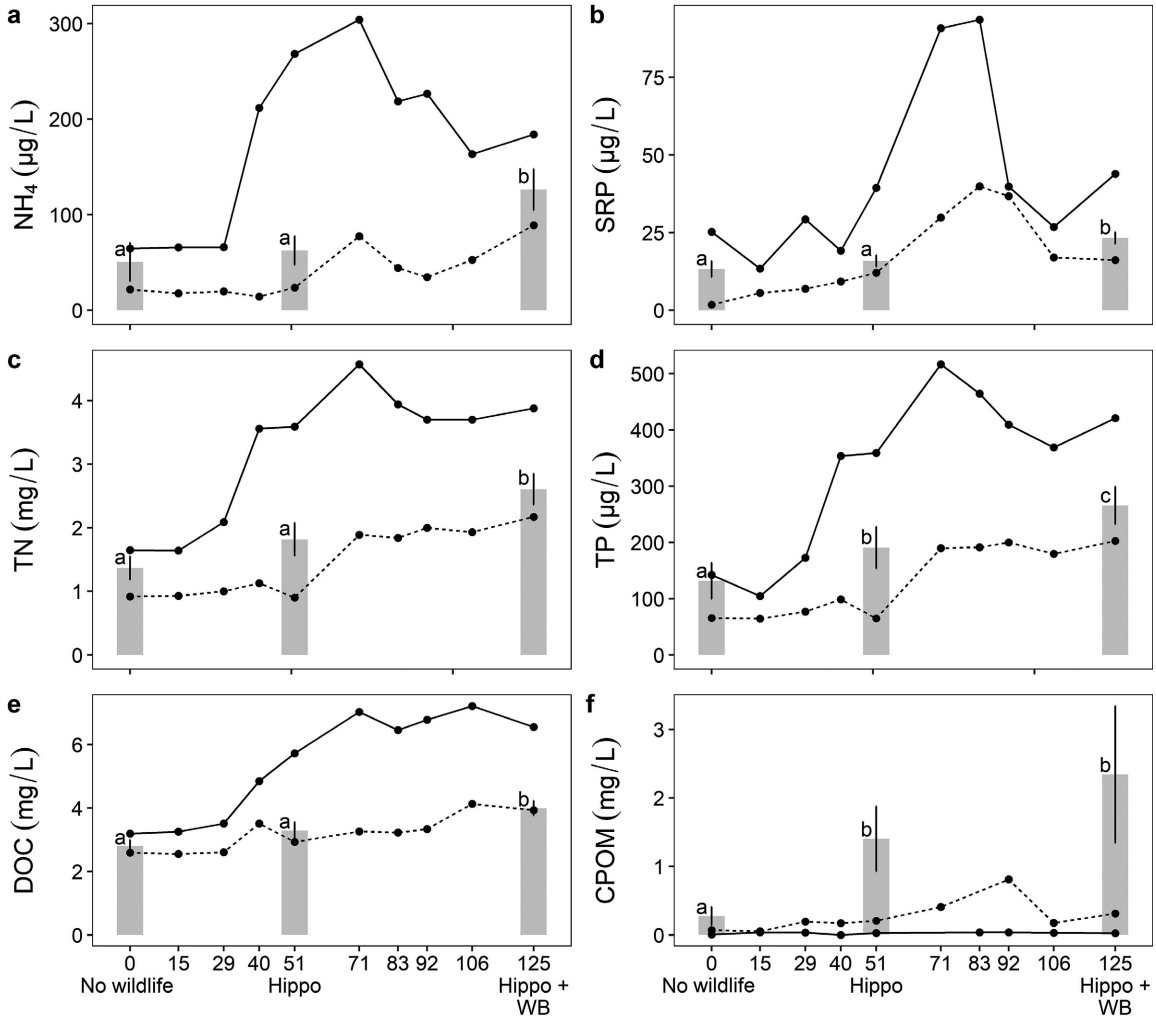

FIG. 4. Concentrations of (a) ammonium, (b) soluble reactive phosphorus, (c) total nitrogen, (d) total phosphorus, (e) dissolved organic carbon, and (f) coarse particulate organic matter at 10 sites from the No Wildlife site (RK 0) to the Hippo + WB site (RK 125) during high flows (dashed line) and low flows (solid line). Concentrations (mean ± SE) for three primary study sites measured over the duration of the study from 2011 to 2014 are shown in bars. Lowercase letters over bars indicate significant differences among group means ($\alpha = 0.05$). Sites are labeled on the *x*-axis as distance in river km from the No Wildlife site. One high coarse particulate organic matter (CPOM) value in both the high (RK 50) and low flow season (RK 43) was removed from panel f for easier visualization.

wildlife inputs in both 2011 (two-way ANOVA, interaction, $F_{10,68} = 5.40$, $P < 0.001$) and 2013 ($F_{12,75} = 3.67$, $P < 0.001$). At the No wildlife site in 2011, *R* on the organic substrate increased significantly relative to the control in response to $NH_4 + PO_4$ and to $NO_3 + PO_4$ (one-way ANOVA, $F_{5,24} = 18.52$, $P < 0.001$; Tukey's HSD, $P = 0.005$ and $P < 0.001$, respectively), but not in response to any of the nutrients alone, indicating N and P colimitation (Appendix S2: Fig. S3). At the No Wildlife site in 2013, *R* increased significantly relative to the control in response to carbon (C), $NH_4 + PO_4$ and PO_4 (one-way ANOVA, $F_{6,21} = 19.22$, $P < 0.001$; Tukey's HSD, $P = 0.006$, $P < 0.001$, and $P < 0.001$, respectively). *R* did not increase in response to NH_4 alone, or in response to PO_4 in combination with NO_3, suggesting primary P limitation with some N and P colimitation along with C limitation (Appendix S2: Fig. S4). There were no significant effects of nutrient treatment on *R* at either the Hippo site or the Hippo + WB site, suggesting no nutrient limitation at those sites.

There was no significant interaction between site and treatment for chl *a* in either 2011 (two-way ANOVA, interaction, $F_{10,71} = 1.92$, $P = 0.057$) or 2013 ($F_{12,77} = 1.02$, $P = 0.444$). Because the interaction was marginally significant in 2011, we proceeded with a one-way ANOVA for that year. At the No Wildlife site in 2011, chl *a* on the inorganic substrate increased significantly relative to the control in response to NH_4 (one-way ANOVA, $F_{5,24} = 3.47$, $P = 0.017$; Tukey's HSD, $P = 0.031$), suggesting some N limitation (Appendix S2: Fig. S3). There were no significant effects of nutrients on chl *a* at either the Hippo site or the Hippo + WB site.

Ecosystem function

Experimental streams.—The rate of biofilm growth in experimental streams was influenced by the presence of wildlife inputs. There was a significant interaction between treatment and time for GPP (lme, interaction effect, $F_{3,32} = 3.03$, $P = 0.044$) and chl *a* (lme, interaction effect,

$F_{3,32}$ = 3.44, P = 0.028; Fig. 5) indicating the rates of change in GPP and chl *a* were different among treatments. The rate of increase was greatest in the Hippo + WB treatment as compared to the Control for both GPP (lstrends pairwise comparison, t_{32} ratio −2.76, P = 0.044) and chl *a* (lstrends pairwise comparison, t_{32} ratio −3.08, P = 0.021).

There was not a significant interaction between treatment and time for *R* (lme, interaction effect, $F_{3,32}$ = 1.07, P = 0.375) or AFDM (lme, interaction effect, $F_{3,32}$ = 1.81, P = 0.165; Fig. 5). Although both *R* and AFDM increased in the Hippo + WB treatment relative to the Control, there was a large amount of variability among replicates that likely precluded statistical significance. High variability was likely due to variations in light exposure across the stream array, despite efforts to minimize this effect; random placement of treatment replicates throughout the array was used to prevent any treatment bias from this effect.

There were differences in standing stock biofilm parameters for all treatments in the final week of the experiment, although none were statistically significant due to small sample sizes and high variability within treatments. However, trends in the data suggest an influence of wildlife inputs on ecological processes and suggest these inputs serve as a subsidy in this ecosystem. Streams with hippo feces had higher *R* than the control streams. Streams with wildebeest tissue had higher GPP and *R* than controls. Streams with both hippo and wildebeest inputs had higher GPP than the summed effects of hippo and wildebeest treatments separately, indicating a synergistic effect.

River biofilms.—GPP (n = 4 per site) increased from the No Wildlife site to the Hippo site but was lowest at the Hippo + WB site (Fig. 6); however, these differences were not significant due to low sample sizes and high variability. Chl *a* (n = 6–8 per site) followed the same pattern, increasing from the No Wildlife site to the Hippo site (not significant), then decreasing from the Hippo site to the Hippo + WB site (one-way ANOVA, $F_{2,19}$ = 9.44, P = 0.001; Tukey's HSD P = 0.001; Fig. 6). There was also a significant difference in chl *a* when comparing by site and season (one-way ANOVA, $F_{3,18}$ = 5.99, P = 0.005). The Hippo + WB site had significantly lower chl *a* than the Hippo site both when carcasses were present (Tukey's HSD, P = 0.015) and when they were not (Tukey's HSD, P = 0.009); however, there was no difference between the Hippo + WB site with and without carcasses (Tukey's HSD, P = 0.996).

Both R (n = 4 per site) and AFDM (n = 6–7 per site) also increased from the No Wildlife site to the Hippo site (not significant). However, *R* and AFDM were very similar between the Hippo site and the Hippo + WB site.

Water column.—GPP rates in the water column were so low that we could not accurately measure GPP or *R* during our 2–4 h incubations. Chl *a*, AFDM, and BOD all differed significantly by site (Table 3, Appendix S2: Fig. S5). Both chl *a* and AFDM increased significantly from the No Wildlife site to the Hippo site and from the Hippo site to the Hippo + WB site (although this was marginally significant for AFDM, P = 0.050; Table 3). BOD increased significantly from the No Wildlife site to the Hippo + WB site (Table 3).

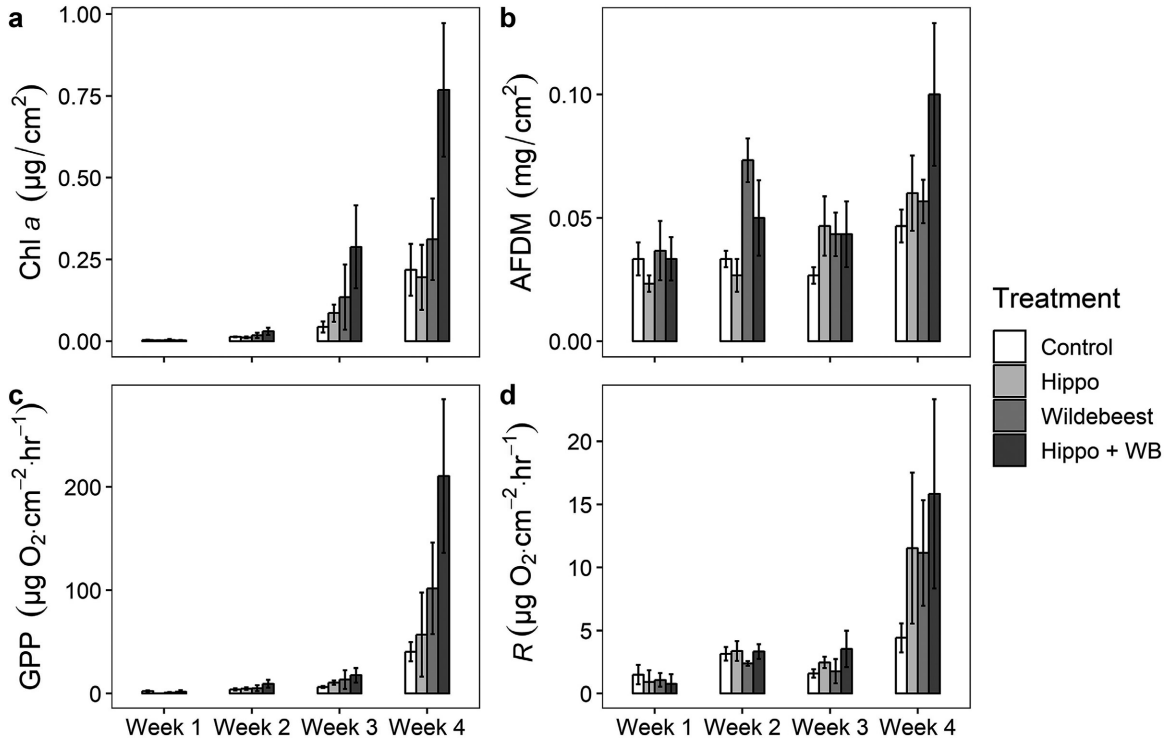

FIG. 5. Mean values (± SE) of (a) chlorophyll *a*, (b) ash-free dry mass, (c) gross primary production, and (d) respiration on ceramic tiles in experimental stream channels over a 4-week period in response to four treatments: control, addition of 10 g fresh hippo feces (Hippo), addition of 10 g fresh wildebeest muscle (Wildebeest), or addition of both 10 g hippo feces and 10 g wildebeest tissue (Hippo + WB).

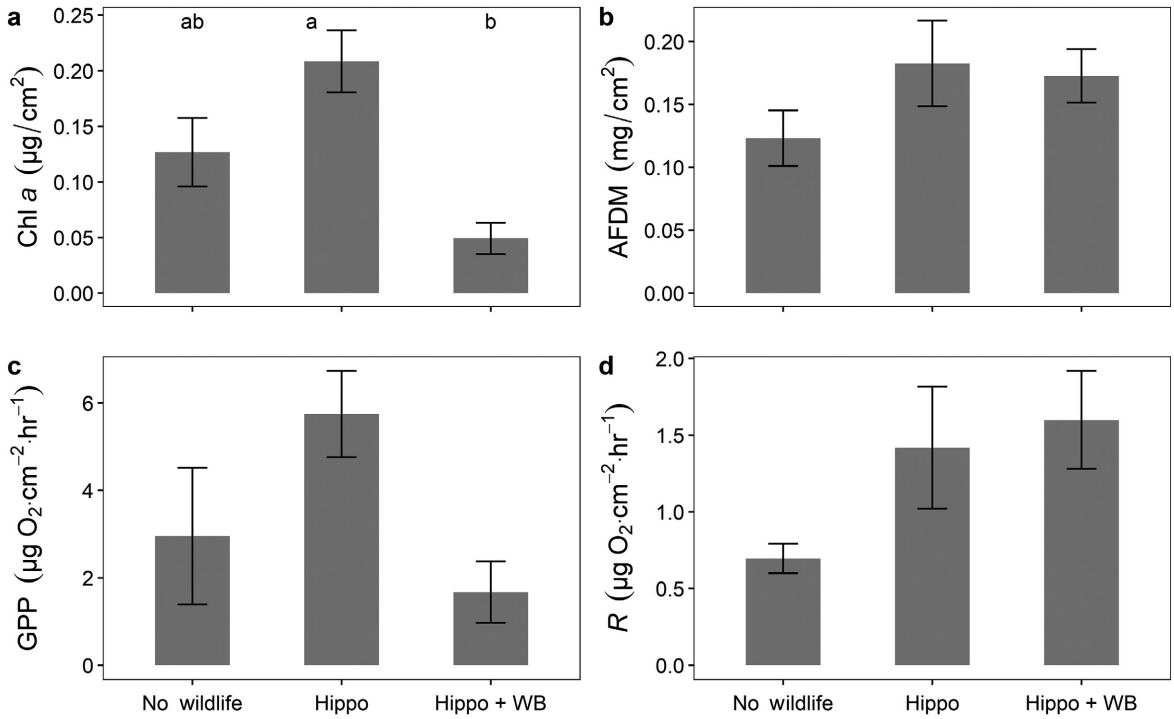

FIG. 6. Mean values (± SE) of (a) chlorophyll *a*, (b) ash-free dry mass, (c) gross primary production, and (d) respiration on ceramic tiles at the No Wildlife, Hippo, and Hippo + WB sites in the Mara River from 2012 to 2014.

DISCUSSION

Differences in the magnitude, stoichiometry, and bioavailability of hippo and wildebeest inputs interact with one another and with discharge to mediate the influence of these inputs on carbon and nutrient concentrations and ecosystem function in the Mara River. Hippo inputs are primarily soluble N and particulate C and they increase NH_4, TP, and CPOM in the river. In contrast, wildebeest carcasses are high in organic N and P and they increase NH_4, SRP, and TP. Increased nutrient concentrations from hippo inputs reduce nutrient limitation of autotrophs and heterotrophs on riverine benthic biofilms. Wildebeest carcasses do not appear to have any additional effect on nutrient limitation, possibly due to saturation of nutrients due to hippo inputs. In experimental streams, wildebeest inputs increased biofilm GPP more than hippo inputs, and there was a synergistic effect when hippo feces and wildebeest carcass tissue were added together, leading to a large increase in GPP. Results from the experimental streams differ from the in situ pattern where biofilm GPP increased from the No Wildlife site to the Hippo site, but decreased from the Hippo site to the Hippo + WB site. This different pattern in the river could be due to increased light limitation, higher frequency of scouring floods, or increased grazing by aquatic insects and fishes at the Hippo + WB site.

Hippos provide subsidies to the Mara River in the form of urine and feces. Hippo urine acts as a daily source of soluble N in the river (Table 1; Subalusky et al. 2015), which likely explains the increase in ammonium flux from the No Wildlife site to the Hippo + WB site, even when wildebeest carcasses were absent (Appendix S2: Table S2; Fig. 3). Hippo feces, which are essentially partially digested grass clippings, provide a large input of particulate C to the river every day. These particles can be measured in the water column of the river as coarse particulate organic matter (CPOM), and CPOM concentrations increased from the No Wildlife site to the Hippo + WB site (Tables 2, 3). Because of its particulate nature, transport of hippo feces downstream is dependent on river velocity (a function of discharge). As such, during low discharge seasons or in river sections with low velocity (i.e., pools), hippo feces settle and accumulate on the river bottom, which was evident in the lower concentrations of CPOM during low flows compared to high flows (Fig. 4). This pattern contrasted with that for dissolved carbon and nutrients, which became much more concentrated at low discharge (Fig. 4). Chamber measurements demonstrate that high concentrations of feces can leach large amounts of ammonium, but leaching occurs predominantly within the first 24 h (Fig. 2). After this initial leaching period, deposited feces likely serve as a largely refractory source of carbon on the river bottom. Decomposition of fresh hippo feces occurs over 80 d, but this rate can be slightly longer (92 d) if the feces were first aged, suggesting feces deposited on land and exposed to rain and sun before being washed into the river may decline in lability (Appendix S2: Fig. S2). Hippo feces in the Mara River are functionally similar to leaf litter in headwater streams, which typically leach a small amount of nutrients relatively quickly and leave a large amount of relatively refractory carbon that decomposes slowly (Webster and Benfield 1986, Webster et al. 1999, Newcomer et al. 2012). However, the continued addition of nutrients via hippo urine and wildebeest carcasses may help facilitate decomposition of fecal carbon (Kominoski et al. 2015, Rosemond et al. 2015). Aged hippo feces in the presence of wildebeest tissue decomposed in only

76 d. Both C and nutrient inputs from hippos appear to alleviate nutrient limitation of biofilms. Autotrophs were N limited and heterotrophs were N and P colimited and C limited at the No Wildlife site, however, there was no carbon or nutrient limitation downstream of hippo inputs (Appendix S2; Figs. S3, S4).

Wildebeest carcasses provide a subsidy to the Mara that is very high in N and P relative to C (Table 1) (Subalusky et al. 2017). Although much of the P is stored in bone that decomposes over years, muscle tissue is high in N and P and decomposes over days to weeks (Subalusky et al. 2017). Chamber measurements demonstrated that carcass soft tissue rapidly leaches N, P, and C (in the form of bioavailable dissolved organic carbon; Fig. 2). Although dissolution of N and P levels off over 1–3 d, dissolved C concentrations continue to increase over time. These inputs were reflected in a 143% increased flux of NH_4 at the Hippo + WB site when carcasses were present in the river compared to the same site when carcasses were not present (although this was not significant), and a significantly increased flux of NH_4, SRP, and TP at the Hippo + WB site when carcasses were present compared to the No Wildlife site (Appendix S2: Table S2; Fig. 3). The Hippo + WB site overall had significantly higher concentrations of NH_4, SRP, TN, TP, and DOC compared to the Hippo site, which may reflect the additional inputs by hippos as well as the influence of wildebeest carcasses (Tables 2, 3). Wildebeest carcasses have a similar influence on nutrient dynamics in the river as salmon carcasses do in headwater streams, which cause large but short-lived increases in NH_4 and SRP (Janetski et al. 2009, Naiman et al. 2009). However, salmon carcasses also tend to increase NO_3 and have a minimal influence on DOC, whereas wildebeest carcasses had no effect on NO_3 but did increase DOC. Furthermore, the high P concentration and slow decomposition rate of wildebeest bones (Subalusky et al. 2017) likely lead to a longer-term subsidy that continues to influence biogeochemical cycles in the Mara River long after the soft tissues of the carcasses are gone. This finding is similar to the effects of bones that have been documented for ungulate carcasses on land (Bump et al. 2009) and whale carcasses in the ocean (Bennett et al. 1994, Smith and Baco 2003). Although wildebeest inputs significantly increase nutrient and carbon concentrations in the river, they do not influence nutrient limitation, possibly because hippo inputs saturate the Mara with N and P (Appendix S2: Figs. S3, S4).

Measurement of C and nutrient fluxes at our primary study sites provided an opportunity to investigate whether spatial patterns observed in the river were consistent with the estimated quantity of wildlife inputs from previous studies (Appendix S1; Subalusky et al. 2015, 2017). CPOM in the Mara River is primarily composed of hippo feces (Subalusky et al. 2017). Our estimates of dry matter inputs from hippos are nearly twice as high as the daily net CPOM flux at the Hippo site (with values from the No Wildlife site subtracted) and 1.5–4.5 times higher than the daily net CPOM flux at the Hippo + WB site (depending on whether carcasses were present). These data indicate that the increase in CPOM can be accounted for by the combination of the spatial pattern of hippos and hippo inputs. The discrepancies in estimated inputs and measured flux suggest we could be overestimating hippo feces inputs, but it is more likely that we are underestimating CPOM flux in the river, as a large amount of hippo feces is stored in the river at low and medium discharge and only flushed through the system during floods, when hippo feces transport can exceed base flow concentrations by several orders of magnitude (Dutton et al. 2018*b*). Our estimate of N inputs from hippos was 99% of daily net TN flux at the Hippo site and 51% at the Hippo + WB site when carcasses were absent. Our estimate of hippo P inputs was 47% of daily net TP flux at the Hippo site and 55% at the Hippo + WB site. Seventy percent of N and 30% of P are loaded through urine, so they follow different dynamics than C inputs from hippo feces. The lower proportion of flux accounted for by estimates of wildlife inputs at the Hippo + WB site may be due to the influence of the Talek River sub-catchment, which contains high densities of livestock and a growing human population and contributes around 50% of the suspended sediments downstream (Dutton et al. 2013, 2018*a*). At the Hippo + WB site when carcasses were present, our estimate of C inputs from wildebeest was 93% of daily net DOC flux. Our estimates of N and P inputs from both hippos and wildebeest were 31% of net TN flux and 16% of daily TP flux. These differences may be partially driven by several high values in measurements of riverine flux. If we instead compare wildlife N and P inputs to the median of measurements of daily net flux at this site, wildlife inputs account for 82% of TN and 52% of TP. Overall, our estimates of hippo and wildebeest inputs are similar in many respects to our estimates of C, N, and P flux, highlighting the role that hippo and wildebeest inputs play in carbon and nutrient dynamics in this system. Differences between estimated wildlife inputs and measured riverine flux may be due to assumptions made in the estimation of inputs and/or to biogeochemical transformations that occur in hippo and carcass aggregations that may lead to atmospheric loss, particularly during low discharge (Subalusky et al. 2015, 2017, Dutton et al. 2018*b*). These differences also highlight the potentially important role of other wildlife and human activities on the landscape, particularly in the Talek River sub-catchment (Dutton et al. 2013, 2018*a*).

Our experimental stream study demonstrated that wildlife inputs influence biofilm growth and productivity in different ways. Hippo inputs increased both GPP and *R* relative to controls, although the increase in *R* was about four times greater than that of GPP (Fig. 5), suggesting that hippo inputs had a larger influence on heterotrophic than autotrophic activity. Wildebeest inputs increased GPP approximately four times greater than hippo inputs, and they increased *R* by approximately the same amount (Fig. 5), indicating a larger net and relative impact on autotrophic activity than hippo inputs. Together, the two inputs had a synergistic effect on primary production. Biofilm chl *a* and GPP increased at a significantly faster rate in streams with both hippo and wildebeest inputs compared to controls, and these effects were greater than the additive effects of hippo or wildebeest inputs alone. Hippo and wildebeest inputs together also increased R relative to controls, although by less than the additive effects of each input alone.

In the Mara River, biofilm chl *a*, GPP, and *R* increased from the No Wildlife site to the Hippo site, and increases

were greatest for *R*, suggesting hippo inputs increase both autotrophic and heterotrophic production but may favor heterotrophs (Fig. 6). However, GPP was lower at the Hippo + WB site than at the upstream sites, while *R* remained high, suggesting high levels of hippo inputs in conjunction with wildebeest inputs strongly favored heterotrophic biofilms and may result in declines in benthic autotrophic activity. In contrast, chl *a* in the water column increased from the No Wildlife site to the Hippo + WB site, suggesting increasing wildlife inputs increase water column productivity (Appendix S2: Fig. S3).

Our results for GPP were quite different in the experimental streams compared to the whole river. Experimental streams with both hippo feces and wildebeest tissue had the highest GPP, but river sites downstream of hippo inputs had the highest GPP while those downstream of both hippo and wildebeest inputs had lower GPP. We propose several, nonexclusive hypotheses for these differences.

First, increased light limitation in the river due to increasing turbidity from up- to downstream could limit GPP at the most downstream site. Turbidity increases from a mean of 266 NTU at the No Wildlife site to a mean of 440 NTU at the Hippo + WB site. This pattern is partially due to the influence of hippos, as hippo feces comprise approximately 11% of suspended solids in the river and hippos stir up sediments through bioturbation (Dutton et al. 2013, 2018*a*). In the Colorado River, primary production was not measurable when turbidity exceeded 200 NTUs (Hall et al. 2015). However, turbidity also increased from the No Wildlife site to the Hippo site, and GPP increased as well, indicating that other factors influence primary production patterns in the basin. Light limitation may also result from shading of benthic biofilms by hippo feces that settle directly on the river bottom. A recent study found that mats of hippo feces that can accumulate during low flows are associated with lower levels of benthic production (Dawson et al. 2016). Moderate levels of hippo inputs, as observed at the Hippo site, may stimulate primary production, but the high levels of hippo inputs above the most downstream site may actually limit primary production due to decreased light availability via these mechanisms.

Second, a higher frequency of scouring floods at the Hippo + WB site, due to the influence of the Talek River sub-catchment (Dutton et al. 2018*a*), may reduce GPP at this site. Research has shown that floods are likely to decrease GPP through scouring of biofilms, but they may increase *R* due to the resuspension of sediments (Tank et al. 2010, Reisinger et al. 2017). Frequent high discharge events at the most downstream site may contribute to lower GPP but elevated rates of heterotrophic activity.

Third, inputs may increase secondary production and thereby increase top-down control of benthic biofilms as a result of grazing by aquatic insects and fishes. The biomass of aquatic insects and fishes increases from the No Wildlife to the Hippo + WB site (*unpublished data*), and isotope data suggest that much of the assimilated diet of insects and fishes at the most downstream site is composed of hippo feces and wildebeest tissue (Masese et al. 2015, 2018, Subalusky et al. 2017). These data suggest that animal inputs in the Mara River may increase secondary production, which could in turn decrease primary production through grazing. This hypothesis is consistent with observations from the Kuparuk River, Alaska, where nutrient additions initially led to increases in primary production that eventually declined due to subsequent increases in grazer production (Peterson et al. 1993), and a body of theory that predicts that increasing magnitude of resource subsidies can strengthen top-down effects on food webs (Huxel and McCann 1998, Leroux and Loreau 2008). The degree to which primary vs. secondary consumers are utilizing animal inputs in the Mara River remains an open question that has important implications for food web structure and ecosystem function.

Conclusion

Our research demonstrates that wildlife inputs can influence nutrient concentrations, nutrient limitation, and ecosystem function in a large African river. In addition, our data demonstrate that different forms of wildlife input interact with one another and with river discharge to influence ecosystem dynamics. Small to moderate inputs by hippos can increase autotrophy, likely due to the high concentrations of inorganic nutrients associated with excretion. However, large inputs by hippos may limit primary production and increase heterotrophic activity, and this may be especially pronounced during low discharge. Carcass inputs are high in essential nutrients that typically limit autotrophs and heterotrophs in riverine ecosystems, and these types of inputs can increase autotrophy in certain conditions. In the Mara River, carcasses may actually stimulate the decomposition of the large amounts of particulate carbon associated with hippo feces and further promote heterotrophic activity, similar to what has been shown when nutrients are added to forested headwater streams with large amounts of allochthonous carbon (Kominoski et al. 2015, Rosemond et al. 2015).

Our research informs our understanding of ecosystems where large wildlife plays an important role (Naiman and Rogers 1997, Schmitz et al. 2014, Malhi et al. 2016), and provides a baseline for comparison with systems where wildlife has disappeared or been replaced by cattle or humans (Belsky et al. 1999, Harris et al. 2009, Gill 2014, Moss 2015, Bakker et al. 2016). Understanding interactions between animal inputs and discharge is particularly important for predicting the consequences of altered river hydrology that may occur in the Mara region due to changes such as increased water abstraction, hydropower development, and climate change (Walters and Post 2011, McClain 2013, Larsen et al. 2016). Although the Mara river represents an end member of river ecosystem studies due to its substantial wildlife inputs, historic range maps of hippos and historical accounts of large migratory animals similar to wildebeest (e.g., American bison) suggest these types of dynamics were not unique in recent history (Isenberg 2000, Saindon 2003). This study helps broaden our understanding of the range of ways rivers function, and the influence large wildlife may have on those dynamics (Tank et al. 2008, Hoellein et al. 2013, Moss 2015).

Acknowledgments

We thank Brian Heath and the Mara Conservancy for hosting us during our research, Paul Geemi for data collection in the field,

Mara Conservancy rangers for their assistance in the field, the Mara River Water Resource User's Association for hosting our experimental streams, and our colleagues at National Museums of Kenya for their assistance with this research. We also thank two anonymous reviewers for constructive input that greatly improved our manuscript. Our research was conducted in affiliation with the National Museums of Kenya under research permit number NCST/RCD/12B/012/36 from the Kenya National Commission for Science, Technology, and Innovation. Funding for this research was provided by the Lee S. Pierce ('82) Fund and the Chair's Fund from Yale's Department of Ecology and Evolutionary Biology, the Yale Institute for Biospheric Studies, the Robert and Patricia Switzer Foundation, the National Geographic Society Committee for Research and Exploration, and the National Science Foundation (DEB 1354053, 1354062, and 1753727).

Literature Cited

Anderson, W. B., D. A. Wait, and P. Stapp. 2008. Resources from another space and time: responses to pulses in a spatially subsidized system. Ecology 89:660–670.

APHA. 2006. Standard methods for the examination of water and wastewater. American Public Health Association, American Water Works Association, Water Environment Federation, Washington, D.C., USA.

Atkinson, C. L., K. A. Capps, A. T. Rugenski, and M. J. Vanni. 2016. Consumer-driven nutrient dynamics in freshwater ecosystems: from individuals to ecosystems. Biological Reviews 92:2003–2023.

Bakker, E. S., J. L. Gill, C. N. Johnson, F. W. M. Vera, C. J. Sandom, G. P. Asner, and J.-C. Svenning. 2016. Combining paleodata and modern exclosure experiments to assess the impact of megafauna extinctions on woody vegetation. Proceedings of the National Academy of Sciences USA 113:847–855.

Belsky, A. J., A. Matzke, and S. Uselman. 1999. Survey of livestock influences on stream and riparian ecosystems in the western United States. Journal of Soil and Water Conservation 54:419–431.

Bennett, B. A., C. R. Smith, B. Glaser, and H. L. Maybaum. 1994. Faunal community structure of a chemoautotrophic assemblage on whale bones in the deep northeast Pacific Ocean. Marine Ecology Progress Series 108:205–223.

Bump, J. K., C. R. Webster, J. A. Vucetich, R. O. Peterson, J. M. Shields, and M. D. Powers. 2009. Ungulate carcasses perforate ecological filters and create biogeochemical hotspots in forest herbaceous layers allowing trees a competitive advantage. Ecosystems 12:996–1007.

Childress, E. S., J. D. Allan, and P. B. McIntyre. 2014. Nutrient subsidies from iteroparous fish migrations can enhance stream productivity. Ecosystems 17:522–534.

Dawson, J., D. Pillay, P. J. Roberts, and R. Perissinotto. 2016. Declines in benthic macroinvertebrate community metrics and microphytobenthic biomass in an estuarine lake following enrichment by hippo dung. Scientific Reports 6:37359.

Dechant-Boaz, D. 1982. Modern riverine taphonomy: its relevance to the interpretation of Plio-Pleistocene hominid paleoecology in the Omo Basin, Ethiopia. Dissertation. University of California, Berkeley, California, USA.

Dinno, A. 2016. dunn.test: Dunn's test of multiple comparisons using rank sums. R package version 1.3.2. https://CRAN.R-project.org/package=dunn.test

Dutton, C., S. Anisfeld, and H. Ernstberger. 2013. A novel sediment fingerprinting method using filtration: application to the Mara River, East Africa. Journal of Soils and Sediments 13:1708–1723.

Dutton, C. L., A. L. Subalusky, S. C. Anisfeld, L. Njoroge, E. J. Rosi, and D. M. Post. 2018*a*. The influence of a semi-arid subcatchment on suspended sediments in the Mara River, Kenya. PLoS ONE 13:e0192828.

Dutton, C. L., A. L. Subalusky, S. K. Hamilton, E. J. Rosi, and D. M. Post. 2018*b*. Organic matter loading by hippopotami causes subsidy overload resulting in downstream hypoxia and fish kills. Nature Communications 9:1951.

Ellis, P. S., A. M. H. Shabani, B. S. Gentle, and I. D. McKelvie. 2011. Field measurement of nitrate in marine and estuarine waters with a flow analysis system utilizing on-line zinc reduction. Talanta 84:98–103.

Eltringham, S. K. 1999. The hippos. A&C Black Publishers, London, UK.

Gibson, C. A., and J. L. Meyer. 2007. Nutrient uptake in a large urban river. Journal of the American Water Resources Association 43:576–587.

Gill, J. L. 2014. Ecological impacts of the late Quaternary megaherbivore extinctions. New Phytologist 201:1163–1169.

Hall, R. O., Jr., C. B. Yackulic, T. A. Kennedy, M. D. Yard, E. J. Rosi-Marshall, N. Voichick, and K. E. Behn. 2015. Turbidity, light, temperature, and hydropeaking control primary productivity in the Colorado River, Grand Canyon. Limnology and Oceanography 60:512–526.

Harris, G., S. Thirgood, J. G. C. Hopcraft, J. P. G. M. Cromsigt, and J. Berger. 2009. Global decline in aggregated migrations of large terrestrial mammals. Endangered Species Research 7:55–76.

Herschy, R. W. 1998. Velocity-area method. Pages 668–670 *in* R. W. Herschy and R. W. Fairbridge, editors. Encyclopedia of hydrology and water resources. Springer, Dordrecht, The Netherlands.

Hoellein, T. J., J. L. Tank, J. J. Kelly, and E. J. Rosi-Marshall. 2010. Seasonal variation in nutrient limitation of microbial biofilms colonizing organic and inorganic substrata in streams. Hydrobiologia 649:331–345.

Hoellein, T. J., D. A. Bruesewitz, and D. C. Richardson. 2013. Revisiting Odum (1956): a synthesis of aquatic ecosystem metabolism. Limnology and Oceanography 58:2089–2100.

Hoffman, C. M. 2007. Geospatial mapping and analysis of water availability-demand-use within the Mara River Basin. Florida International University, Miami, Florida, USA.

Holm, S. 1979. A simple sequentially rejective multiple test procedure. Scandinavian Journal of Statistics 6:65–70.

Holmes, R. M., A. Aminot, R. Kérouel, B. A. Hooker, and B. J. Peterson. 1999. A simple and precise method for measuring ammonium in marine and freshwater ecosystems. Canadian Journal of Fisheries and Aquatic Sciences 56:1801–1808.

Holm-Hansen, O. 1978. Chlorophyll a determination: improvements in methodology. Oikos 30:438–447.

Holtgrieve, G. W., and D. E. Schindler. 2011. Marine-derived nutrients, bioturbation, and ecosystem metabolism: reconsidering the role of salmon in streams. Ecology 92:373–385.

Hopcraft, J. G. C., A. R. E. Sinclair, R. M. Holdo, E. Mwangomo, S. Mduma, S. Thirgood, M. Borner, J. M. Fryxell, and H. Olff. 2013. Why are wildebeest the most abundant herbivore in the Serengeti ecosystem? Serengeti IV: sustaining biodiversity in a coupled human–natural system. University of Chicago Press, Chicago, Illinois, USA.

Huxel, G. R., and K. McCann. 1998. Food web stability: the influence of trophic flows across habitats. American Naturalist 152:460–469.

Isenberg, A. C. 2000. The destruction of the bison. Cambridge University Press, Cambridge, Massachusetts, USA.

Janetski, D. J., D. T. Chaloner, S. D. Tiegs, and G. A. Lamberti. 2009. Pacific salmon effects on stream ecosystems: a quantitative synthesis. Oecologia 159:583–595.

Kanga, E. M., J. O. Ogutu, H. Olff, and P. Santema. 2011. Population trend and distribution of the vulnerable common hippopotamus *Hippopotamus amphibius* in the Mara Region of Kenya. Oryx 45:20–27.

Kanga, E. M., J. O. Ogutu, H.-P. Piepho, and H. Olff. 2013. Hippopotamus and livestock grazing: influences on riparian vegetation and facilitation of other herbivores in the Mara Region of Kenya. Landscape and Ecological Engineering 9:47–58.

Kitchell, J. F., R. V. Oneill, D. Webb, G. W. Gallepp, S. M. Bartell, J. F. Koonce, and B. S. Ausmus. 1979. Consumer regulation of nutrient cycling. BioScience 29:28–34.

Kitchell, J. F., D. E. Schindler, B. R. Herwig, D. M. Post, M. H. Olson, and M. Oldham. 1999. Nutrient cycling at the landscape

scale: the role of diel foraging migrations by geese at the Bosque del Apache National Wildlife Refuge, New Mexico. Limnology and Oceanography 44:828–836.
Kominoski, J. S., A. D. Rosemond, J. P. Benstead, V. Gulis, J. C. Maerz, and D. W. P. Manning. 2015. Low-to-moderate nitrogen and phosphorus concentrations accelerate microbially driven litter breakdown rates. Ecological Applications 25:856–865.
Larsen, S., J. D. Muehlbauer, and E. Marti. 2016. Resource subsidies between stream and terrestrial ecosystems under global change. Global Change Biology 22:2489–2504.
Lenth, R. V. 2016. Least-squares means: the R package lsmeans. Journal of Statistical Software 69:1–33.
Leroux, S. J., and M. Loreau. 2008. Subsidy hypothesis and strength of trophic cascades across ecosystems. Ecology Letters 11:1147–1156.
Levi, P. S., J. L. Tank, S. D. Tiegs, D. T. Chaloner, and G. A. Lamberti. 2013. Biogeochemical transformation of a nutrient subsidy: salmon, streams, and nitrification. Biogeochemistry 113:643–655.
Malhi, Y., C. E. Doughty, M. Galetti, F. A. Smith, J.-C. Svenning, and J. W. Terborgh. 2016. Megafauna and ecosystem function from the Pleistocene to the Anthropocene. Proceedings of the National Academy of Sciences USA 113:838–846.
Marcarelli, A. M., C. V. Baxter, M. M. Mineau, and R. O. Hall. 2011. Quantity and quality: unifying food web and ecosystem perspectives on the role of resource subsidies in freshwaters. Ecology 92:1215–1225.
Marczak, L. B., R. M. Thompson, and J. S. Richardson. 2007. Meta-analysis: trophic level, habitat, and productivity shape the food web effects of resource subsidies. Ecology 88:140–148.
Masese, F. O., K. G. Abrantes, G. M. Gettel, S. Bouillon, K. Irvine, and M. E. McClain. 2015. Are large herbivores vectors of terrestrial subsidies for riverine food webs? Ecosystems 18:686–706.
Masese, F. O., K. G. Abrantes, G. M. Gettel, K. Irvine, S. Bouillon, and M. E. McClain. 2018. Trophic structure of an African savanna river and organic matter inputs by large terrestrial herbivores: a stable isotope approach. Freshwater Biology. https://doi.org/10.111/fwb.13163
Mati, B. M., S. Mutie, H. Gadain, P. Home, and F. Mtalo. 2008. Impacts of land-use/cover changes on the hydrology of the transboundary Mara River, Kenya/Tanzania. Lakes & Reservoirs: Research & Management 13:169–177.
McCauley, D. J., et al. 2015. Carbon stable isotopes suggest that hippopotamus-vectored nutrients subsidize aquatic consumers in an East African river. Ecosphere 6:art52.
McClain, M. E. 2013. Balancing water resources development and environmental sustainability in Africa: a review of recent research findings and applications. Ambio 42:549–565.
McClain, M. E., et al. 2003. Biogeochemical hot spots and hot moments at the interface of terrestrial and aquatic ecosystems. Ecosystems 6:301–312.
McIntyre, P. B., A. S. Flecker, M. J. Vanni, J. M. Hood, B. W. Taylor, and S. A. Thomas. 2008. Fish distributions and nutrient cycling in streams: can fish create biogeochemical hotspots? Ecology 89:2335–2346.
Menninger, H. L., M. A. Palmer, L. S. Craig, and D. C. Richardson. 2008. Periodical cicada detritus impacts stream ecosystem metabolism. Ecosystems 11:1306–1317.
Meyer, J. L., and E. T. Schultz. 1985. Migrating haemulid fishes as a source of nutrients and organic matter on coral reefs. Limnology and Oceanography 30:146–156.
Moss, B. 2015. Mammals, freshwater reference states, and the mitigation of climate change. Freshwater Biology 60:1964–1976.
Naiman, R. J., and K. H. Rogers. 1997. Large animals and system level characteristics in river corridors. BioScience 47:521–529.
Naiman, R. J., J. M. Helfield, K. K. Bartz, D. C. Drake, and J. M. Honea. 2009. Pacific salmon, marine-derived nutrients, and the characteristics of aquatic and riparian ecosystems. Pages 395–425 *in* A. Haro, K. L. Smith, R. A. Rulifson, C. M. Moffitt, R. J. Klauda, M. J. Dadswell, R. A. Cunjak, J. E. Cooper, K. L. Beal, and T. S. Avery, editors. Challenges for diadromous fishes in a dynamic global environment. American Fisheries Society, Bethesda, Maryland, USA.
Newcomer, T. A., S. S. Kaushal, P. M. Mayer, A. R. Shields, E. A. Canuel, P. M. Groffman, and A. J. Gold. 2012. Influence of natural and novel organic carbon sources on denitrification in forest, degraded urban, and restored streams. Ecological Monographs 82:449–466.
Paetzold, A., M. Lee, and D. M. Post. 2008. Marine resource flows to terrestrial arthropod predators on a temperate island: the role of subsidies between systems of similar productivity. Oecologia 157:653–659.
Peterson, B. J., et al. 1993. Biological responses of a tundra river to fertilization. Ecology 74:653–672.
Pinheiro, J., D. Bates, S. DebRoy, D. Sarkar, and R. C. Team. 2016. nlme: linear and nonlinear mixed effects models. https://CRAN.R-project.org/package=nlme
Polis, G. A., and S. D. Hurd. 1996. Linking marine and terrestrial food webs: allochthonous input from the ocean supports high secondary productivity on small islands and coastal land communities. American Naturalist 147:396–423.
Polis, G. A., W. B. Anderson, and R. D. Holt. 1997. Toward an integration of landscape and food web ecology: the dynamics of spatially subsidized food webs. Annual Review of Ecology and Systematics 28:289–316.
Post, D. M., and A. W. Walters. 2009. Nutrient excretion rates of anadromous alewives during their spawning migration. Transactions of the American Fisheries Society 138:264–268.
Post, D. M., J. P. Taylor, J. F. Kitchell, M. H. Olson, D. E. Schindler, and B. R. Herwig. 1998. The role of migratory waterfowl as nutrient vectors in a managed wetland. Conservation Biology 12:910–920.
Power, M. E., A. Sun, G. Parker, W. E. Dietrich, and J. T. Wootton. 1995. Hydraulic food-chain models. BioScience 45:159–167.
R Core Team. 2018. R: a language and environment for statistical computing. R Foundation for Statistical Computing, Vienna, Austria. www.r-project.org
Regester, K. J., and M. R. Whiles. 2006. Decomposition rates of salamander (*Ambystoma maculatum*) life stages and associated energy and nutrient fluxes in ponds and adjacent forest in Southern Illinois. Copeia 2006:640–649.
Reisinger, A. J., E. J. Rosi, H. A. Bechtold, T. R. Doody, S. S. Kaushal, and P. M. Groffman. 2017. Recovery and resilience of urban stream metabolism following Superstorm Sandy and other floods. Ecosphere 8:e01776.
Richardson, J. S., Y. X. Zhang, and L. B. Marczak. 2010. Resource subsidies across the land-freshwater interface and responses in recipient communities. River Research and Applications 26:55–66.
Roberts, B. J., and R. W. Howarth. 2006. Nutrient and light availability regulate the relative contribution of autotrophs and heterotrophs to respiration in freshwater pelagic ecosystems. Limnology and Oceanography 51:288–298.
Roman, J., and J. J. McCarthy. 2010. The whale pump: marine mammals enhance primary productivity in a coastal basin. PLoS ONE 5:e13255.
Rosemond, A. D., J. P. Benstead, P. M. Bumpers, V. Gulis, J. S. Kominoski, D. W. P. Manning, K. Suberkropp, and J. B. Wallace. 2015. Experimental nutrient additions accelerate terrestrial carbon loss from stream ecosystems. Science 347:1142–1145.
Saindon, R. A. 2003. Explorations into the world of Lewis and Clark. Digital Scanning, Scituate, Massachusetts, USA.
Samways, K. M., and R. A. Cunjak. 2015. Increases in benthic community production and metabolism in response to marine-derived nutrients from spawning Atlantic salmon (*Salmo salar*). Freshwater Biology 60:1647–1658.
Schmitz, O. J., et al. 2014. Animating the carbon cycle. Ecosystems 17:344–359.
Sitters, J., C. L. Atkinson, N. Guelzow, P. Kelly, and L. L. Sullivan. 2015. Spatial stoichiometry: cross-ecosystem material flows and their impact on recipient ecosystems and organisms. Oikos 124:920–930.
Smith, C. R., and A. R. Baco. 2003. Ecology of whale falls at the deep-sea floor. Oceanography and Marine Biology 41:311–354.

Stears, K., D. J. McCauley, J. C. Finlay, J. Mpemba, I. T. Warrington, B. M. Mutayoba, M. E. Power, T. E. Dawson, and J. S. Brashares. 2018. Effects of the hippopotamus on the chemistry and ecology of a changing watershed. Proceedings of the National Academy of Sciences USA 11:E5028–E5037.

Subalusky, A. L., C. L. Dutton, E. J. Rosi-Marshall, and D. M. Post. 2015. The hippopotamus conveyor belt: vectors of carbon and nutrients from terrestrial grasslands to aquatic systems in sub-Saharan Africa. Freshwater Biology 60:512–525.

Subalusky, A. L., C. L. Dutton, E. J. Rosi, and D. M. Post. 2017. Annual mass drownings of the Serengeti wildebeest migration influence nutrient cycling and storage in the Mara River. Proceedings of the National Academy of Sciences USA 114:7647–7652.

Subalusky, A. L., and D. M. Post. 2018. Context dependency of animal resource subsidies. Biological Reviews. https://doi.org/10.1111/brv.12465

Tank, J. L., M. J. Bernot, and E. J. Rosi-Marshall. 2007. Nitrogen limitation and uptake. Pages 213–238 *in* F. R. Hauer and G. A. Lamberti, editors. Methods in stream ecology. Elsevier Academic Press, New York, New York, USA.

Tank, J. L., E. J. Rosi-Marshall, M. A. Baker, and R. O. Hall. 2008. Are rivers just big streams? A pulse methods to quantify nitrogen demands in a large river. Ecology 89:2935–2945.

Tank, J. L., E. J. Rosi-Marshall, N. A. Griffiths, S. A. Entrekin, and M. L. Stephen. 2010. A review of allochthonous organic matter dynamics and metabolism in streams. Journal of the North American Benthological Society 29:118–146.

Tank, J. L., A. J. Reisinger, and E. J. Rosi. 2017. Nutrient limitation and uptake. Pages 147–171 *in* F. R. Hauer and G. A. Lamberti, editors. Methods in stream ecology. Elsevier Academic Press, New York, New York, USA.

Taylor, B. W., C. F. Keep, R. O. Hall, B. J. Koch, L. M. Tronstad, A. S. Flecker, and A. J. Ulseth. 2007. Improving the fluorometric ammonium method: matrix effects, background fluorescence, and standard additions. Journal of the North American Benthological Society 26:167–177.

Tiegs, S. D., P. S. Levi, J. Ruegg, D. T. Chaloner, J. L. Tank, and G. A. Lamberti. 2011. Ecological effects of live salmon exceed those of carcasses during an annual spawning migration. Ecosystems 14:598–614.

Vanni, M. J. 2002. Nutrient cycling by animals in freshwater ecosystems. Annual Review of Ecology and Systematics 33:341–370.

Walters, A. W., and D. M. Post. 2011. How low can you go? Impacts of a low-flow disturbance on aquatic insect communities. Ecological Applications 21:163–174.

Walters, A. W., R. T. Barnes, and D. M. Post. 2009. Anadromous alewives (*Alosa pseudoharengus*) contribute marine-derived nutrients to coastal stream food webs. Canadian Journal of Fisheries and Aquatic Sciences 66:439–448.

Webster, J. R., and E. F. Benfield. 1986. Vascular plant breakdown in fresh-water ecosystems. Annual Review of Ecology and Systematics 17:567–594.

Webster, J. R., E. F. Benfield, T. P. Ehrman, M. A. Schaeffer, J. L. Tank, J. J. Hutchens, and D. J. D'Angelo. 1999. What happens to allochthonous material that falls into streams? A synthesis of new and published information from Coweeta. Freshwater Biology 41:687–705.

Wider, R. K., and G. E. Lang. 1982. A critique of the analytical methods used in examining decomposition data obtained from litter bags. Ecology 63:1636–1642.

Wipfli, M. S., J. Hudson, and J. Caouette. 1998. Influence of salmon carcasses on stream productivity: response of biofilm and benthic macroinvertebrates in southeastern Alaska, USA. Canadian Journal of Fisheries and Aquatic Sciences 55:1503–1511.

Witman, J. D., J. C. Ellis, and W. B. Anderson. 2004. The influence of physical processes, organisms, and permeability on cross-ecosystem fluxes. Pages 335–358 *in* G. A. Polis, M. E. Power, and G. R. Huxel, editors. Food webs at the landscape level. University of Chicago Press, Chicago, Illinois, USA.

Young, R. G., and A. D. Huryn. 1996. Interannual variation in discharge controls ecosystem metabolism along a grassland river continuum. Canadian Journal of Fisheries and Aquatic Sciences 53:2199–2211.

Supporting Information

Additional supporting information may be found in the online version of this article at http://onlinelibrary.wiley.com/doi/10.1002/ecy.2509/suppinfo

Data Availability

Data are availability from the Dryad Data Repository: https://doi.org/10.5061/dryad.g886d9v.